

High-Resolution Forecast Models of Water Vapor Over Mountains: Comparison With MERIS and Meteosat Data

Min Zhu, *Member, IEEE*, Geoff Wadge, Rachel J. Holley, Ian N. James, Peter A. Clark, Changgui Wang, and Margaret J. Woodage

Abstract—Propagation delay due to variable tropospheric water vapor (WV) is one of the most intractable problems for radar interferometry, particularly over mountains. The WV field can be simulated by an atmospheric model, and the difference between the two fields is used to correct the radar interferogram. Here, we report our use of the U.K. Met Office Unified Model in a nested mode to produce high-resolution forecast fields for the 3-km-high Mount Etna volcano. The simulated precipitable-water field is validated against that retrieved from the Medium-Resolution Imaging Spectrometer (MERIS) radiometer on the Envisat satellite, which has a resolution of 300 m. Two case studies, one from winter (November 24, 2004) and one from summer (June 25, 2005), show that the mismatch between the model and the MERIS fields (rms = 1.1 and 1.6 mm, respectively) is small. One of the main potential sources of error in the models is the timing of the WV field simulation. We show that long-wavelength upper tropospheric troughs of low WV could be identified in both the model output and Meteosat WV imagery for the November 24, 2004 case and used to choose the best time of model output.

Index Terms—Differential synthetic aperture radar interferometry (DInSAR), Medium Resolution Imaging Spectrometer (MERIS), Meteosat, unified model, water vapor (WV).

I. INTRODUCTION

THE SPATIAL distribution and temporal variation of atmospheric water vapor (WV) is of interest, not only for weather and climate change but also for geodetic measurements. For example, differential synthetic aperture radar interferometry (DInSAR) can measure deformation of the Earth's surface over periods of days to years with millimetric accuracy. In repeat-pass mode, the technique is based on the phase-difference image (interferogram) derived from two SAR acquisitions in different epochs. However, the single largest noise component for DInSAR in most circumstances is the temporal variability of the tropospheric WV field which can cause variable "delays" of radio-wave propagation along the radar line of sight (LOS), generating several centimeters of

pseudo ground motion in the interferogram. Mountainous areas such as volcanoes are particularly susceptible to such noise, due to the complicated interaction between the orography and the atmosphere [1]–[3]. If other error sources are negligible, then the relation among the surface deformation, interferometric phase difference, and difference in tropospheric WV content can be approximately expressed as

$$\delta_{a,b} = \frac{\lambda \times \phi_{a,b}}{4\pi} - (\text{LOSPW}_{a,b} \times Q) \quad (1)$$

where $\delta_{a,b}$ is the surface displacement of point b relative to point a , λ is the radar wavelength, $\phi_{a,b}$ is the interferogram phase difference between a and b in radians, $\text{LOSPW}_{a,b}$ is the difference in precipitable water (PW) between a and b along the two-way radar LOS measured at the epochs of two SAR acquisitions that form the interferogram, and Q is a dimensionless quantity which varies with the mean temperature of the atmosphere [4].

Various statistical and calibratory methods have been proposed to reduce the WV noise in InSAR [5]. However, generally, these methods need either a large archive of SAR data or sufficient independent measurements related to WV delay, so their use has been greatly restricted. Wadge *et al.* [1] reported a more generally applicable approach to this problem. This involved a mesoscale atmospheric numerical model over the 3.3-km-high Mount Etna volcano (Fig. 1) with a cell size of 1.7 km and simplified model physics in which neither cloud nor precipitation are considered. Their models were initialized with either a single radiosonde record or global numerical weather prediction analysis cell data to predict the LOSPW on two SAR acquisition dates. The simulated atmospheric WV information was then used to correct the radar interferogram. After comparing with InSAR and independent global positioning system (GPS)-derived slant wet delay measurements, they found that the general pattern of the atmospheric noise in the interferogram could be captured by the model but with residual errors.

For the purposes of assimilation into forecast models and the study of the hydrological cycle, meteorologists also model the atmospheric WV, validating results with data derived from different kinds of sensors such as radiosonde, GPS, WV radiometer (WVR), and very long baseline interferometry [6]–[8]. The results are sensitive to latitude, altitude, season, and the time of day. The general accuracy of WV models can

Manuscript received June 12, 2006; revised November 6, 2006. This work was supported by the National Environment Research Council under NER/A/S/2003/00470.

M. Zhu, G. Wadge, R. J. Holley, and M. J. Woodage are with the Environmental Systems Science Centre, University of Reading, RG6 6AL Reading, U.K. (e-mail: gw@mail.nerc-essc.ac.uk).

I. N. James and C. Wang are with the Department of Meteorology, University of Reading, RG6 6BB Reading, U.K.

P. A. Clark is with the Joint Centre for Mesoscale Meteorology, Met Office, EX1 3PB Exeter, U.K.

Digital Object Identifier 10.1109/LGRS.2007.895884

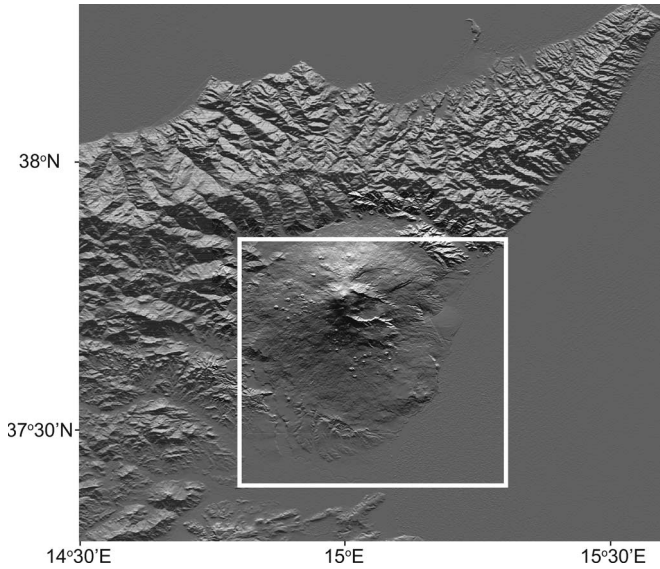


Fig. 1. Shaded relief image of northeastern Sicily. The Etna area is highlighted by the rectangle that defines the area used in the statistical calculations.

be as low as 2–3 mm [root mean-squared (rms) error], which is close to the 1–2 mm accuracy of sensors. Generally, such models are limited by their relatively low spatial resolution (> 7 km) and sparse validation data.

To realize the full potential of a forward atmospheric-model approach for correcting DInSAR, it is important that we provide an accurate representation of the WV field at an appropriate scale. In this letter, we employ the U.K. Met Office Unified Model to do this. We illustrate the results with a winter and a summer simulation of the WV fields over the Mount Etna volcano in Sicily (Fig. 1) that correspond to the times of overpass of the Envisat satellite. The Medium Resolution Imaging Spectrometer (MERIS) instrument on this satellite provides an independent measurement of the PW for comparison purposes. In addition, we show how a time series of geostationary satellite WV imagery (Meteosat-7) can be used in some circumstances to select the appropriate model output.

II. UNIFIED MODEL, MERIS, AND METEOSAT DATA

The model used is the atmospheric module of the U.K. Met Office Unified Model, version 5.5 (hereafter UM). After nearly 15 years of development, the UM has been successfully applied in a wide range of fields from climate modeling and numerical weather prediction to mesoscale modeling [9], [10]. The UM is a nonhydrostatic deep-atmospheric grid-point model with an Arakawa-C grid in the horizontal plane and a terrain-following Charney–Philips grid in the vertical plane. The main variables are the three components of wind, potential temperature, Exner pressure, density, and components of moisture (vapor, cloud water, and cloud ice). Model physics includes land surface (vegetation-cover type, soil temperature, and moisture) and planetary boundary layer (PBL) processes, radiation, cloud microphysics, and convection. For our particular purpose, the model is run in a nested mode with cell sizes of 60, 12, 4, and 1 km, respectively, and with 38 vertical layers (13 layers within the PBL). The outermost domain (60 km) is global. The innermost domain (1 km) covers the whole of Sicily.

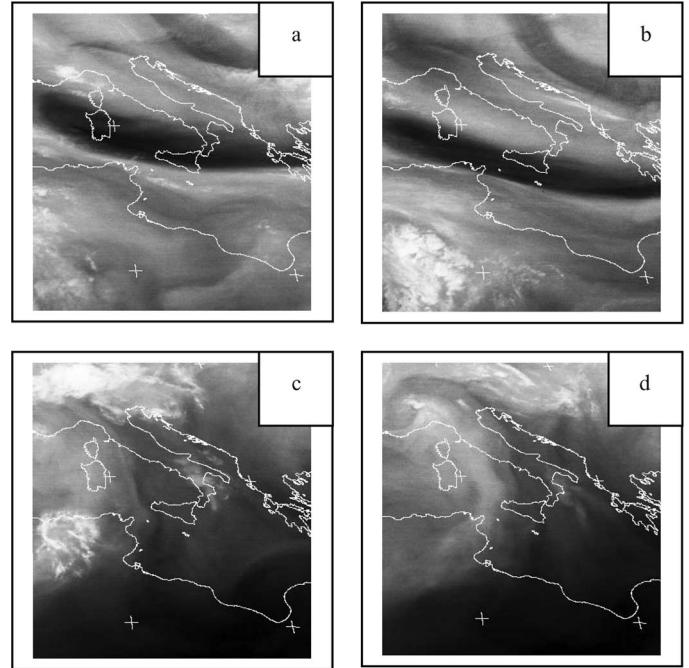


Fig. 2. Meteosat-7 WV channel images of the central Mediterranean with Sicily centrally placed at (a) 0000 UTC and (b) 0900 UTC, November 24, 2004, (c) 0000 UTC and (d) 0900 UTC, June 25, 2005.

A semi-implicit, semi-Lagrangian, and predictor–corrector algorithm is used for model integration. The time step for the 1-km domain is 30 s. The lateral boundary conditions for the 1-km domain are interpolated from the 4-km domain every 15 min. A series of model initialization schemes has been tested, and the preferred schemes start at either 0000 UTC and 0600 UTC (descending pass) or 1200 UTC and 1800 UTC (ascending pass) with the European Centre for Medium-Range Weather Forecasts (ECMWF) global atmospheric analysis (0.5° latitude \times 0.5° longitude). The models are run for a 12-h period, with hourly output, during which the SAR data are acquired at 0911 UTC and 2046 UTC.

The PW data for model validation are retrieved from MERIS near-infrared channels under cloud-free conditions in daytime. MERIS and Advanced SAR (ASAR) are mounted on the same platform of the European Space Agency (ESA) polar-orbiting Envisat satellite, and they can acquire data simultaneously. The MERIS data that we use are full resolution, with a nadir spatial sampling of 260 m across track by 290 m along track, the highest resolution of its kind currently available. The theoretical accuracy of the MERIS PW product is 1.6 mm over land, much less accurate over water [11], and hence, we only use onland MERIS values for comparison. Li *et al.* [12], [13] found a very good correlation among MERIS-, WVR-, and GPS-derived PW fields with a standard deviation of 1.1 mm. MERIS PW fields can have a small wet-bias relative to GPS-derived values [13]. It should be noted that, although MERIS data allow the WV noise from a daytime ASAR interferogram to be calculated, cloud-free conditions for Mount Etna during SAR acquisitions occur only about 10% of the time. The modeled and observed PW are usually interpolated and registered onto a grid of 300-m resolution for comparison. The cloudy areas in the MERIS field are masked.

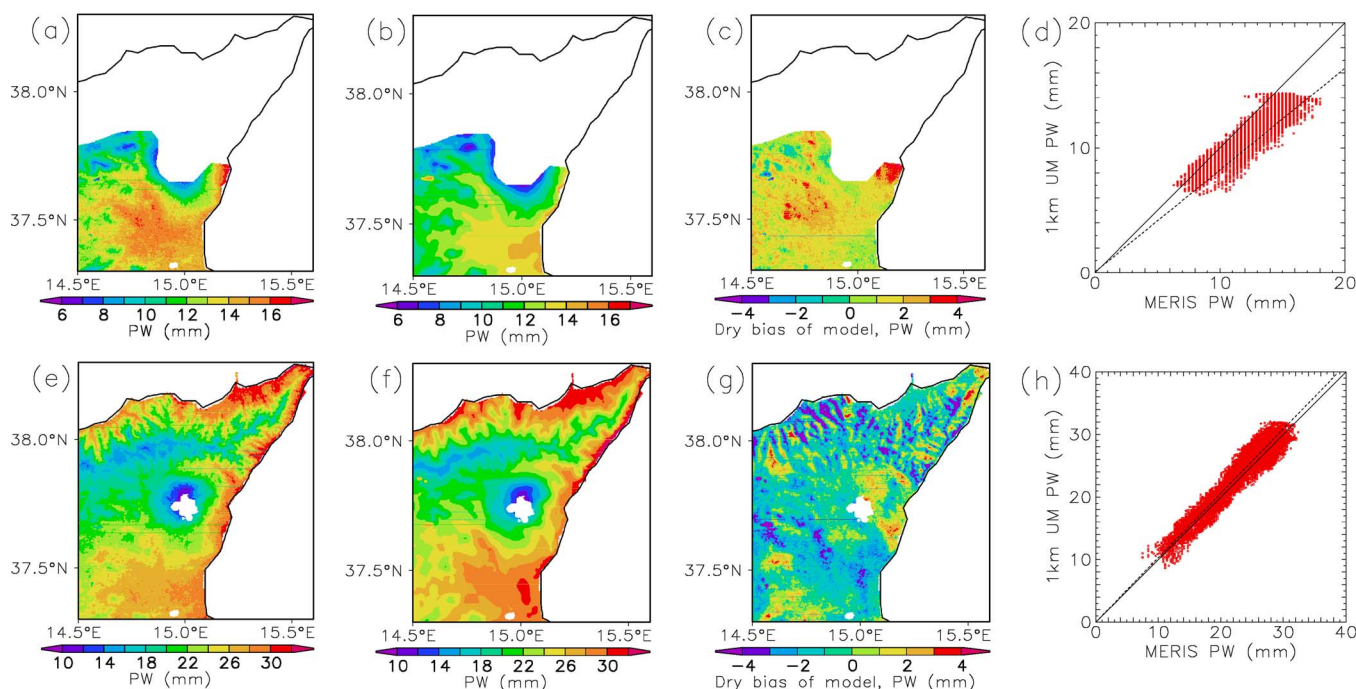


Fig. 3. (a) MERIS-retrieved PW (in millimeters) at 0900 UTC November 24, 2004 (cloud-affected areas are masked as white). (b) The 1-km UM-modeled PW (in millimeters) at 0900 UTC November 24, 2004 (initialized at 0600 UTC). (c) Difference between MERIS and UM-modeled PW (in millimeters). (d) Scatterplot of modeled and observed PW over Etna area (see Fig. 1). Dashed line is the linear fitting line of data points. Number of points = 11 420. bias = 1.4 mm. rms = 1.6 mm. correlation coefficient = 0.93. (e) MERIS-retrieved PW (in millimeters) at 0900 UTC June 25, 2005. (f) The 1-km UM-modeled PW (in millimeters) at 0900 UTC June 25, 2005 (initialized at 0600 UTC). (g) Difference between MERIS and UM-modeled PW (in millimeters). (h) Scatter plot of modeled and observed PW over Etna area. Dashed line is the linear fitting line of data points. Number of points = 15 141. bias = -0.8 mm. rms = 1.60 mm. correlation coefficient = 0.96. The bias is calculated based on MERIS 1-km UM values.

Horizontal moisture gradients, which are common in the atmosphere, can be misrepresented by the atmospheric model because of either poor resolution of initial conditions or model error [3]. The timing of the passage of these moisture gradients can sometimes be constrained by the WV (six to seven micron emission) images acquired by geostationary satellites [14] every 15 min at a spatial resolution of about 4 km in the case of the Meteosat-7 satellite which currently observes the Etna region. Here, we use a time series of these images to detect the passage of any upper troposphere WV troughs (subsidence inversions) over Etna and, by comparison with the equivalent model features, over an area of about 400 km², detect and correct for any mistiming in the UM output. This approach only works if the upper troposphere is sufficiently dry to detect the emission of lower level WV. We use the time of the passage of the trough detected in the Meteosat data, rather than the WV values themselves, although these can be retrieved empirically by calibration with GPS-derived WV data [15].

III. RESULTS

A. November 24, 2004

At 0911 UTC on November 24, 2004, Sicily was marginally influenced by a low-pressure system, and patchy cloud covered the northeast coast as well as the adjacent mountains, although the area to the south and west of Etna was cloud-free. An east-southeast trending WV trough feature crossed the Etna region from north to south during the period of the model runs from 0000 UTC to 1800 UTC (Fig. 2). Fig. 3(a) and (b) shows the MERIS-observed PW and 1-km

UM-modeled (0000 UTC initialization, 0900 UTC output) PW, respectively. The observed PW pattern and its strong correlation with the topography (see Fig. 1) are well simulated. There is a minor dry bias in the model relative to the observations, particularly over the regions to the west of Etna [Fig. 3(c)]. The data sets are compared cellwise in Fig. 3(d) for the area immediately south and west of Etna [Fig. 3(a)]. The MERIS values are, on average, 1.4 mm wetter than those of the UM, the rms difference between the two is 1.6 mm, and the correlation coefficient is 0.93.

Consecutive Meteosat WV channel images showed that an asymmetrical belt of low moisture passed over Sicily from north to south [dark band in Fig. 2(a) and (b)] between 0000 UTC and 1800 UTC. Fig. 4 shows that the minimum of this trough measured by the Meteosat images passed over Etna at about 0500 UTC. The 1-km UM models also successfully captured the passage of this moisture feature. The model initialized at 0000 UTC shows that the Etna-area averaged PW values first decreased from 0000 UTC to 0800 UTC and then increased steadily in the next 4 h (Fig. 4). A model initialized at 0600 UTC also reaches a well-defined minimum at 0800 UTC and rose thereafter (Fig. 4). Thus, the models predict the arrival of this feature over Etna about 3 h later than it was observed to occur. Hence, a better fit to the WV field at the time of the Envisat overpass at 0911 UTC should be obtained from the UM output at 1200 (0900 + 3 h) UTC. Fig. 5 (vertical dashed line) demonstrates that this is the case (as measured against the MERIS WV field) for the bias (reduced from +0.15 to -0.05 mm) and standard deviation (reduced from 0.16 to 0.11 mm) but not for the correlation coefficient (down from

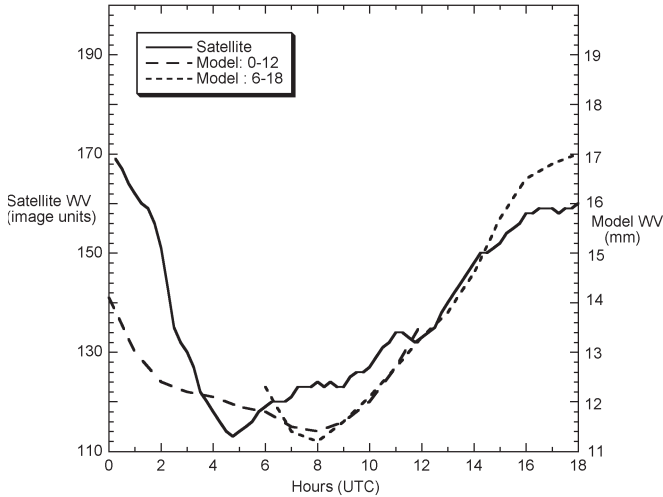


Fig. 4. Temporal comparison of the average UM model WV field output over Etna for models initialized at 0000 UTC and 0600 UTC, with the Meteosat-7 WV channel image brightness values over Etna for November 24, 2004.

0.93 to 0.90). Errors in the initial vertical humidity field of the model have probably caused the correlation coefficient value not to be a maximum at the time of the standard deviation minimum. Note that these model field values come from the run initialized at 0600 UTC.

B. June 25, 2005

This was a day of low winds ($\sim 1 - 3 \text{ m} \cdot \text{s}^{-1}$) over Sicily and a northwest to southeast moisture gradient over the Mediterranean that moved eastward with time [Fig. 2(c) and (d)]. Orographic clouds due to local convection covered the Etna summit and its immediate area at 0911 UTC. Fig. 3(e) and (f) shows the MERIS-observed PW and UM-modeled (0000 UTC initialization, 0900 UTC output) PW for this case. Because of the smoothed orography used in the 1-km model, the model misses the fine structures of the PW field seen in the observed field over the incised northern mountains. A slightly wet bias in the model relative to the observations can be seen west of Etna [Fig. 3(g)]. Otherwise, the model reproduces the observed PW pattern well. The cellwise data plot [Fig. 3(h)] shows that MERIS is 0.8 mm drier than the UM PW; the rms between the two is 1.6 mm, and the correlation coefficient is 0.96.

Unlike the November 24, 2004 case, the Meteosat data for June 25, 2005 show no large well-defined low WV features passing over Etna (Fig. 6). The WV measured in this case is from the moist upper troposphere, which obscures any lower level variability. The UM models (0000 UTC and 0600 UTC initializations) show, generally, high values of PW (relative to the November 24, 2004 case) rising after about 0600 UTC, but there is no prominent low WV trough that can be used to indicate any possible timing offset. Hence, we retain the 0900 UTC UM model output as the best fit. The solid vertical line in Fig. 5 shows that this timing provides the best fits for standard deviation and correlation coefficient, and the bias (-0.1 mm) is close to optimal.

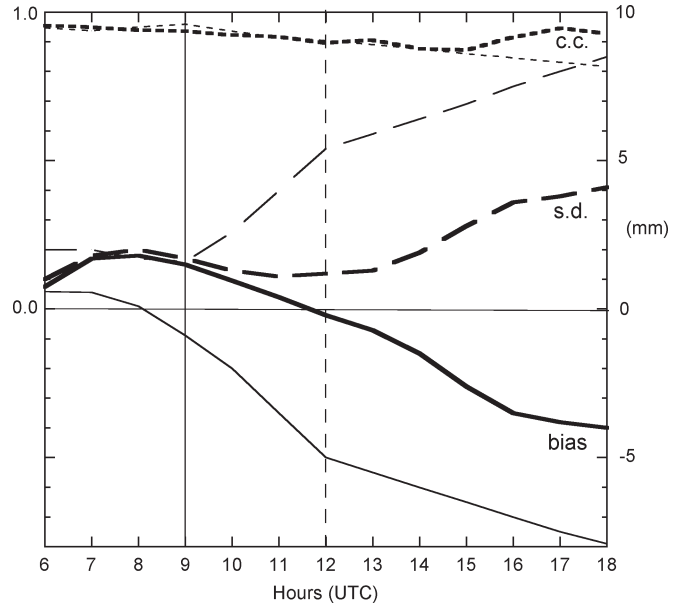


Fig. 5. Temporal statistical comparison between the UM-model WV field values measured on the hour and the observed MERIS WV field values at 0911 UTC for November 24, 2004 (thick lines) and June 25, 2005 (fine lines). The dashed vertical black line is the best fit for November 24, 2004 and the solid vertical black line the best fit for June 25, 2005. The solid curves are bias values (in millimeters), the long dashed curves are standard deviation values (in millimeters), and the short dashed curves are correlation coefficient values.

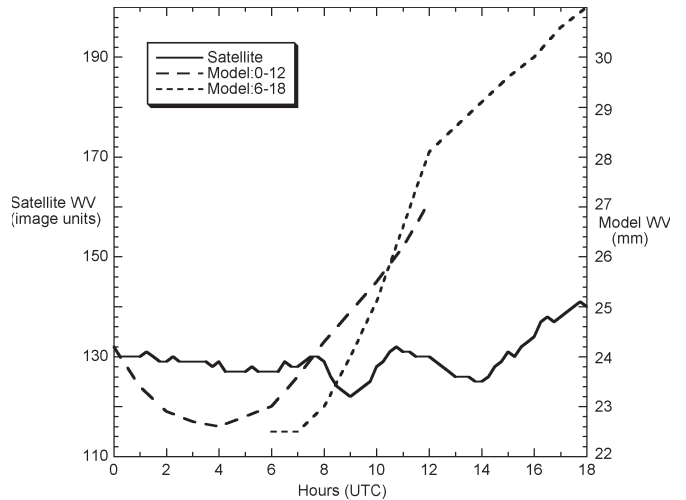


Fig. 6. Temporal comparison of the average UM-model WV field output over Etna for models initialized at 0000 UTC and 0600 UTC, with the Meteosat-7 WV channel image brightness values over Etna for June 25, 2005.

IV. DISCUSSION AND CONCLUSION

The strengths of this approach of forward modeling of the atmosphere for the correction of the WV field effects on InSAR are as follows: 1) the method is potentially applicable anywhere and is independent of the need for data (e.g., GPS, satellite radiometry) other than the freely available global analysis of the atmosphere; 2) it captures the dynamic local features of atmospheric flow over and around mountains and areas of high relief. Over flat or modest-relief terrain, the advantages of 2) largely disappear, but 1) remains.

For the two cases presented here, the model performance is promising, as the mismatch between the UM and MERIS

results is at the approximate level of accuracy of the MERIS data product. Partial (noncloudy) MERIS coverage is still useful for model validation in about half the cases. To improve the noise characteristics of the InSAR data, we use four looks in range and azimuth to give an image resolution of about 100 m. This still leaves a scale mismatch between the InSAR (100 m), model (1 km), and MERIS (300 m) data. In the future, we will increase the UM model data to 300 m over Etna to make the data more closely comparable.

Choosing the best model output to represent the WV field at the time of radar overpass is not always straightforward. A model initialized at 0600 UTC should be able to represent the field at 0911 UTC better than one initialized at 0000 UTC, because more recent observational data have been assimilated into the ECMWF model used for initialization, and the drift of the forward model should be less. Model output that best fits the available MERIS field can be chosen, as in the case of June 25, 2005, which also happens to be the “correct” model run time (0900 UTC). Our demonstrated use of geostationary WV images to correct the timing of the model output of the November 24, 2004 case was dependent on having a suitable WV “feature” within the model space. Note that we only used the temporal information from this time series to effect a correction, not the WV contents themselves.

When it is totally cloudy and no MERIS or other satellite WV field data are available, how could we identify the time of the optimum model field corresponding to the radar overpass? One possibility is to use continuous GPS WV estimates from a site within or near the area covered by the model space to identify the passage of long-wavelength features as we have shown for the Meteosat data. It should also be possible to use the information within the interferograms themselves. By assuming that the ground motion is negligible within a minimum interval for an interferogram (e.g., 35 days for Envisat), analysis of a series of such interferograms may allow the best fit timings for each epoch to be estimated.

ACKNOWLEDGMENT

The authors would like to thank B. W. Atkinson and B. Golding for their reviews of an earlier version of the manuscript. This version benefited from suggestions by three anonymous reviewers. MERIS data for this letter were supplied by ESA (C1P.2880).

REFERENCES

- [1] G. Wadge, P. W. Webley, I. N. James, R. Bingley, A. Dodson, S. Waugh, T. Veneboer, G. Puglisi, M. Mattia, D. Baker, S. C. Edwards, and S. J. Edwards, “Atmospheric models, GPS and InSAR measurements of the tropospheric water vapour field over Mount Etna,” *Geophys. Res. Lett.*, vol. 29, no. 19, pp. 11.1–11.4, 2002. DOI:10.1029/2002GL015159.
- [2] P. W. Webley, R. M. Bingley, A. H. Dodson, G. Wadge, S. J. Waugh, and I. N. James, “Atmospheric water vapour correction to InSAR surface motion measurements on mountains: Results from a dense GPS network on Mount Etna,” *Phys. Chem. Earth*, vol. 27, no. 4, pp. 363–370, 2002.
- [3] P. W. Webley, G. Wadge, and I. N. James, “Determining radio wave delay by non-hydrostatic atmospheric modelling of water vapour over mountains,” *Phys. Chem. Earth*, vol. 29, no. 2/3, pp. 139–148, 2004.
- [4] T. R. Emardson and H. J. P. Derks, “On the relation between the wet delay and the integrated precipitable water vapour in the European atmosphere,” *Meteorol. Appl.*, vol. 7, no. 1, pp. 61–68, Mar. 2000.
- [5] S. Williams, Y. Bock, and P. Fang, “Integrated satellite interferometry: Tropospheric noise, GPS estimates and implications for interferometric synthetic aperture radar products,” *J. Geophys. Res.*, vol. 103, no. B11, pp. 27 051–27 067, 1998.
- [6] S. Hagemann, L. Bengtsson, and G. Gendt, “On the determination of atmospheric water vapour from GPS measurements,” *J. Geophys. Res.*, vol. 108, no. D21, 4678, 2003. DOI:10.1029/2002JD003235.
- [7] D. Behrend, R. Hass, D. Pino, L. P. Gradinarsky, S. J. Keihm, W. Schwarz, L. Cucurull, and A. Rius, “MM5 derived ZWDs compared to observational results from VLBI, GPS AND WVR,” *Phys. Chem. Earth*, vol. 27, no. 4, pp. 301–308, 2002.
- [8] X. H. Yang, B. H. Sass, G. Elgered, J. M. Johansson, and T. R. Emardson, “A comparison of precipitable water vapour estimates by an NWP simulation and GPS observations,” *J. Appl. Meteorol.*, vol. 38, no. 7, pp. 941–956, Jul. 1999.
- [9] T. Davies, M. J. P. Cullen, A. J. Malcolm, M. H. Mawson, A. Staniforth, A. A. White, and N. Wood, “A new dynamical core for the Met Offices global and regional modelling of the atmosphere,” *Q. J. R. Meteorol. Soc.*, vol. 131(B), no. 608, pp. 1759–1782, 2005.
- [10] Met Office, *Unified Model User Guide*, 2004. [Online]. Available: <http://www.cgam.nerc.ac.uk/um/docs/>
- [11] R. Bennartz and J. Fischer, “Retrieval of columnar water vapour over land from back-scattered solar radiation using the Medium Resolution Imaging Spectrometer (MERIS),” *Remote Sens. Environ.*, vol. 78, no. 3, pp. 274–283, Dec. 2001.
- [12] Z. H. Li, J. P. Muller, P. Cross, P. Albert, T. Hewison, R. Watson, J. Fischer, and R. Bennartz, “Validation of MERIS near IR water vapour retrievals using MWR and GPS measurements,” in *Proc. MERIS User Workshop*, 2003.
- [13] Z. H. Li, J. P. Muller, P. A. Cross, P. Albert, P. Fischer, and R. Bennartz, “Assessment of the potential of MERIS near-infrared water vapour products to correct ASAR interferometric measurements,” *Int. J. Remote Sens.*, vol. 27, no. 1/2, pp. 349–365, 2006.
- [14] M. J. Bader, G. S. Forbes, J. R. Grant, R. B. E. Lilley, and A. J. Waters, *Images in Weather Forecasting*. Cambridge, U.K.: Cambridge Univ. Press, 1995, p. 499.
- [15] R. Hanssen, *Radar Interferometry: Data Interpretation and Error Analysis*. Norwell, MA: Kluwer, 2001, pp. 226–237.